Science Advances
AAAS

Supplementary Materials for

Intrinsically stretchable electronics with ultrahigh deformability to monitor dynamically moving organs

Shaolei Wang, Yuanyuan Nie, Hangyu Zhu, Yurui Xu, Shitai Cao, Jiaxue Zhang, Yanyan Li, Jianhui Wang, Xinghai Ning*, Desheng Kong*

*Corresponding author. Email: dskong@nju.edu.cn (D.K.); xning@nju.edu.cn (X.N.)

Published 30 March 2022, *Sci. Adv.* **8**, eabl5511 (2022)
DOI: 10.1126/sciadv.abl5511

The PDF file includes:

Other Supplementary Material for this manuscript includes the following:

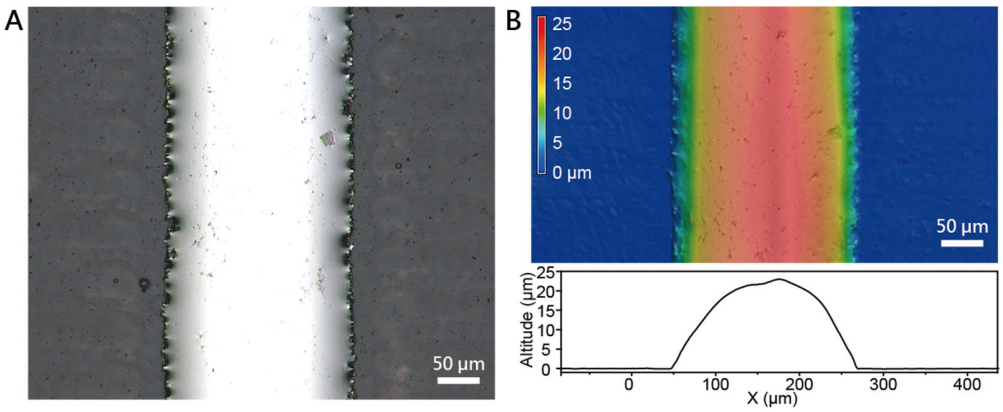

Fig. S1.

Cross section of liquid metal features. (**A**) Optical image of a 200 µm-wide liquid metal track. (**B**) Corresponding topographic image to reveal the cross-sectional morphology.

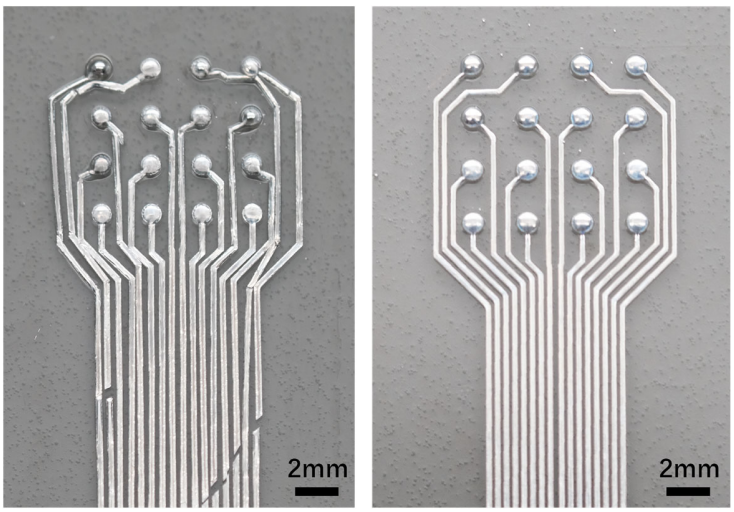

Fig. S2.

Spin-cast SEBS layer for encapsulation. Optical image of liquid metal features after spin-coating SEBS solutions in toluene (left) and hexane (right), respectively. The liquid metal feature is damaged by toluene solution to trigger excessive swelling of the underneath substrate. In contrast, the liquid metal pattern remains intact by using a slow swelling solution in hexane.

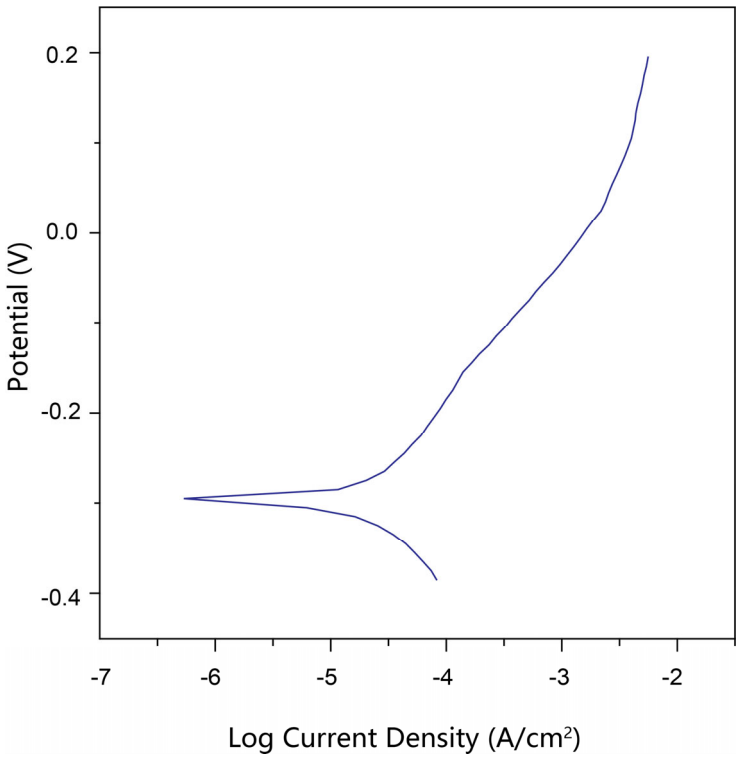

Fig. S3.

Tafel plot of liquid metal feature in PBS solution. The linear sweep voltammetry is carried out at a scan rate of 1 mV/s.

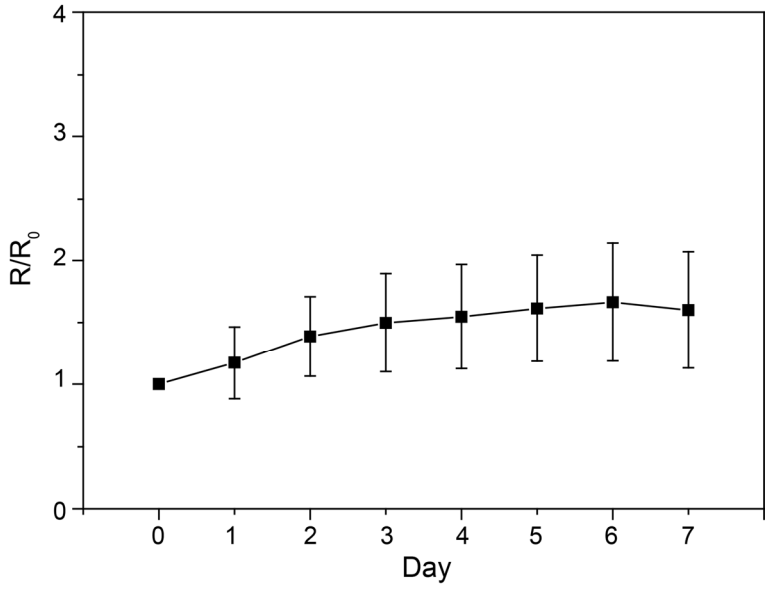

Fig. S4.

Stability of encapsulated liquid metal features in PBS solution. Normalized resistance as a function of storage time.

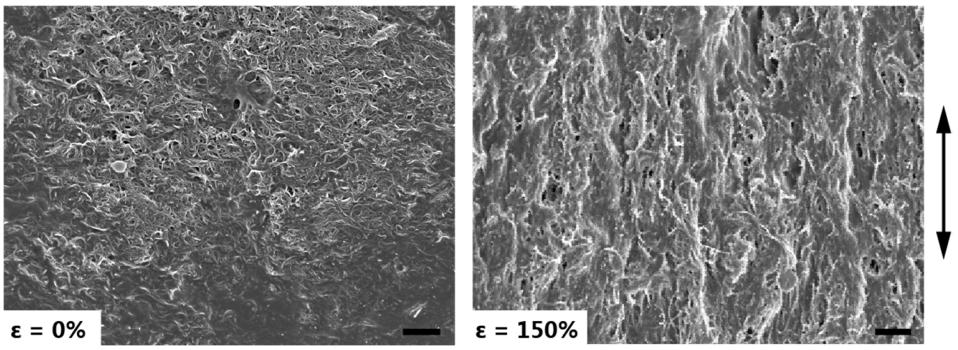

Fig. S5.

Microstructures of the conductive nanocomposite. SEM images acquired at 0% (left) and 150% (right) tensile strains. The arrow indicates the stretching direction.

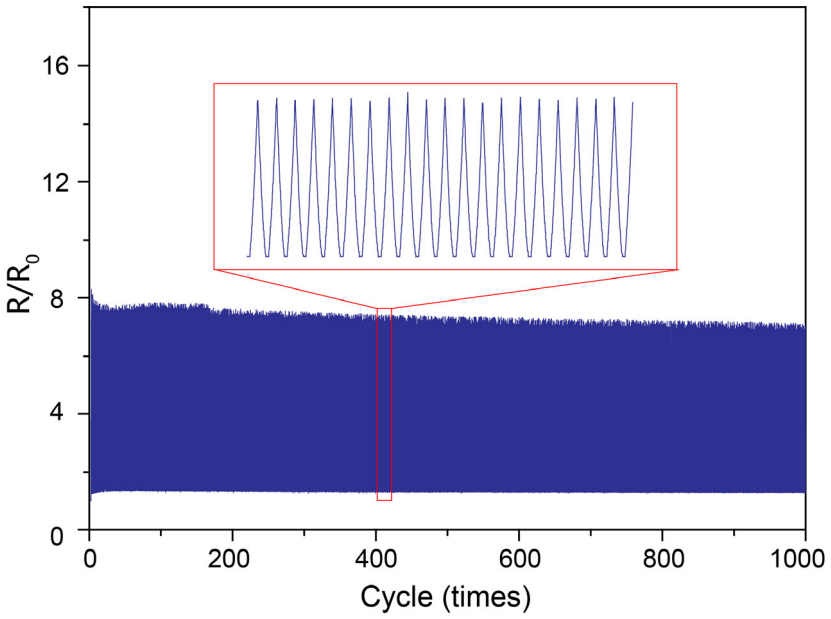

Fig. S6.

Electromechanical durability of liquid metal features. Change in normalized resistance over 1000 stretch-relaxation cycles to 300 % strain.

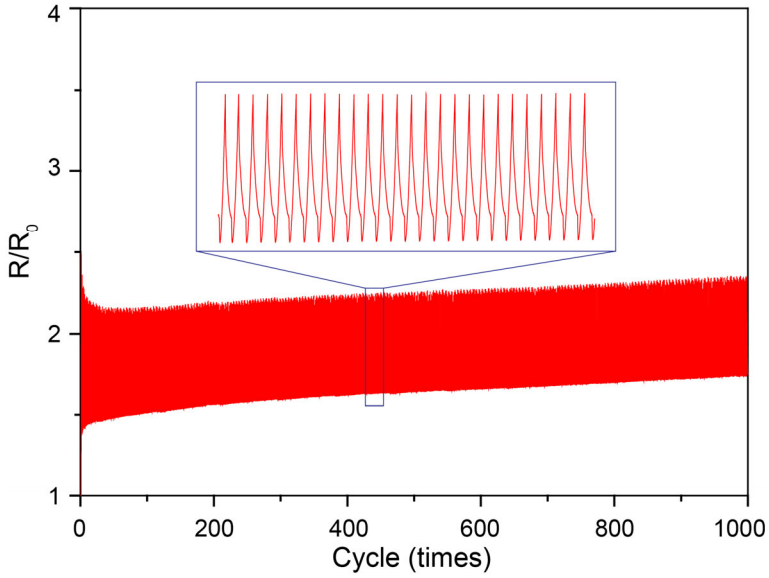

Fig. S7.

Electromechanical durability of conductive nanocomposite features. Change in normalized resistance over 1000 stretch-relaxation cycles to 40 % strain.

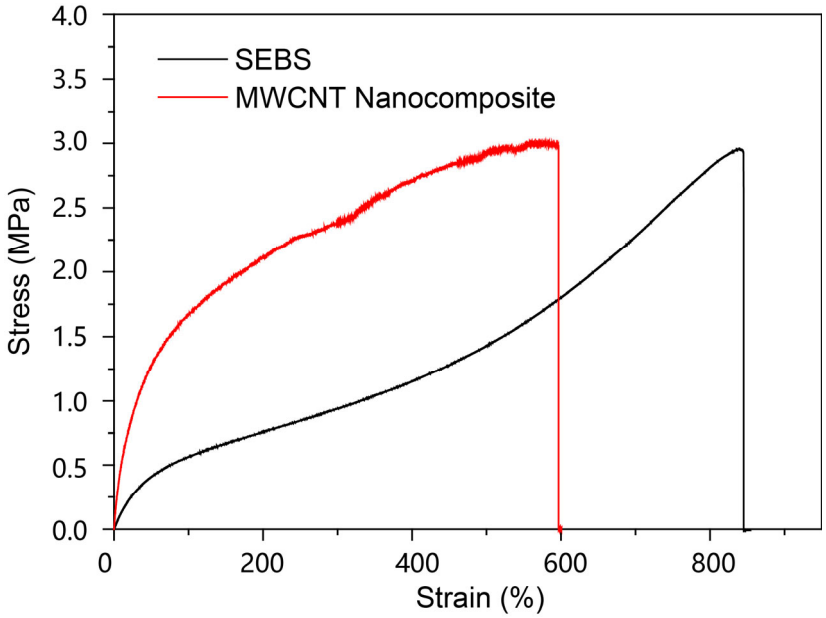

Fig. S8.

Stress-strain curves of SEBS elastomer and conductive nanocomposite under uniaxial tensile deformations. SEBS elastomer has a Young's modulus of 1.3 MPa and a fracture strain of ~850%. Conductive nanocomposite has a Young's modulus of 5.1 MPa and a fracture strain of ~600%.

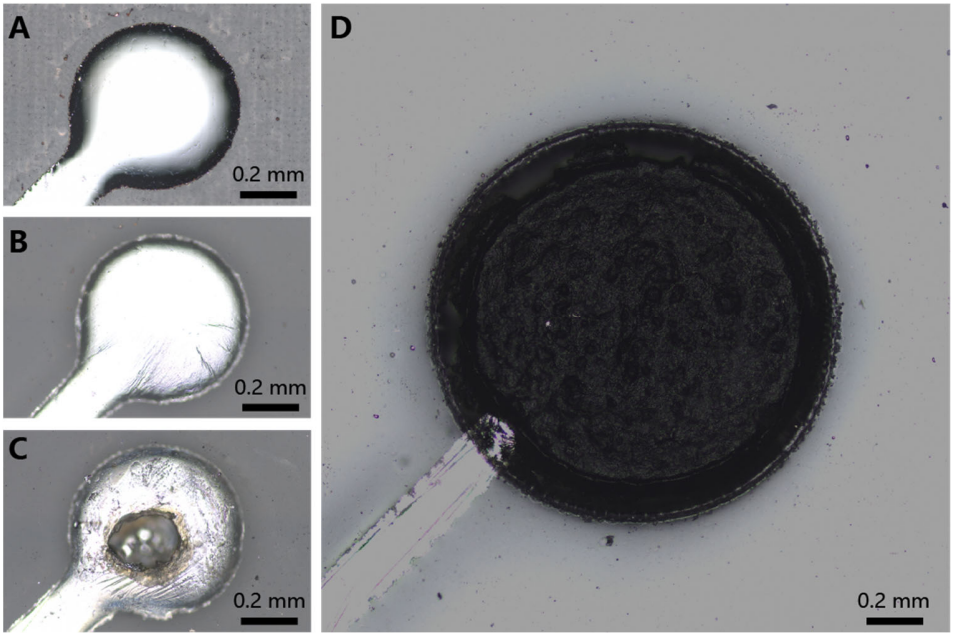

Fig. S9.

Fabrication procedures to create sensing electrodes on liquid metal contact pads. Optical microscopy images are acquired at each step involving the formation of liquid metal patterns (**A**), the encapsulation with spin-casted elastomer (**B**), the creation of VIAs by laser ablation (**C**), and the preparation of printed conductive nanocomposite electrodes (**D**).

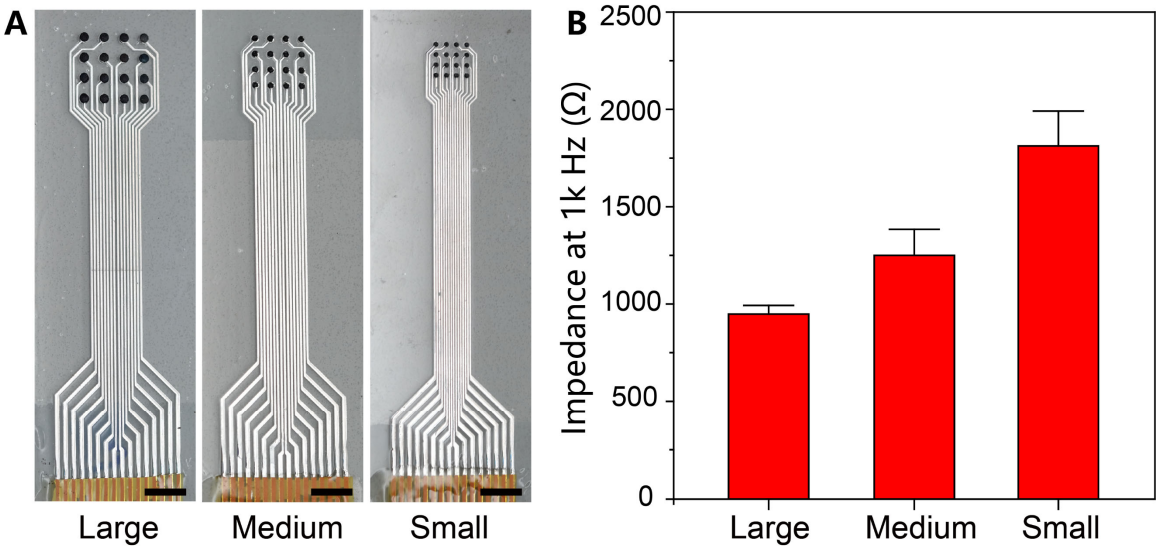

Fig. S10.

Stretchable electronic patches of different sizes. (**A**) Optical images of three electronic patches. Scale bar: 5mm. The diameter of an individual sensing electrode is 1200, 900, and 600 μm, respectively. (**B**) Impedance at 1 kHz of an individual sensing channel on the large, medium, and small electronic patches.

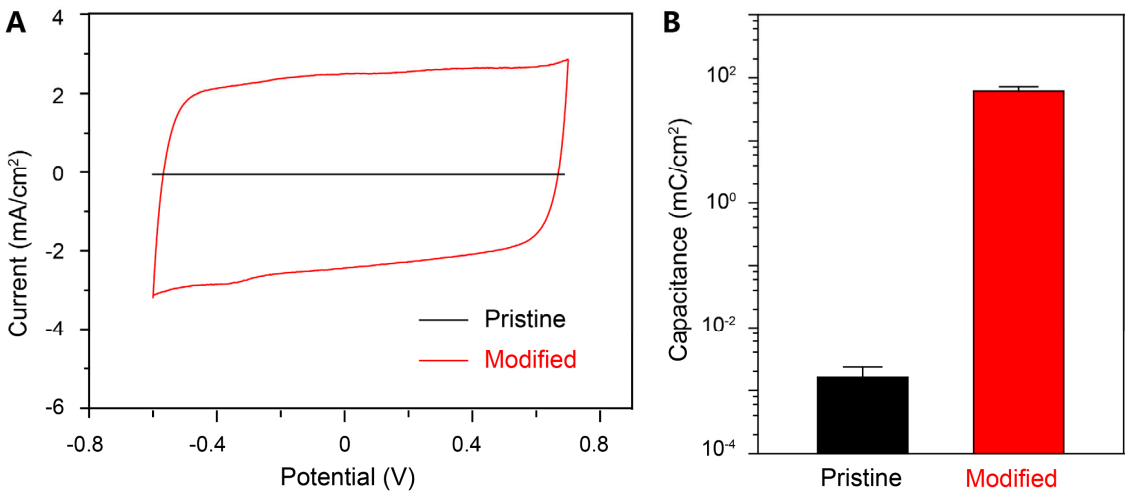

Fig. S11.

Capacitance of individual sensing electrodes. (**A**) Cyclic voltammograms of a representative sensing channel before and after modifications with PEDOT: PSS interface layer. (**B**) Corresponding specific capacitance values.

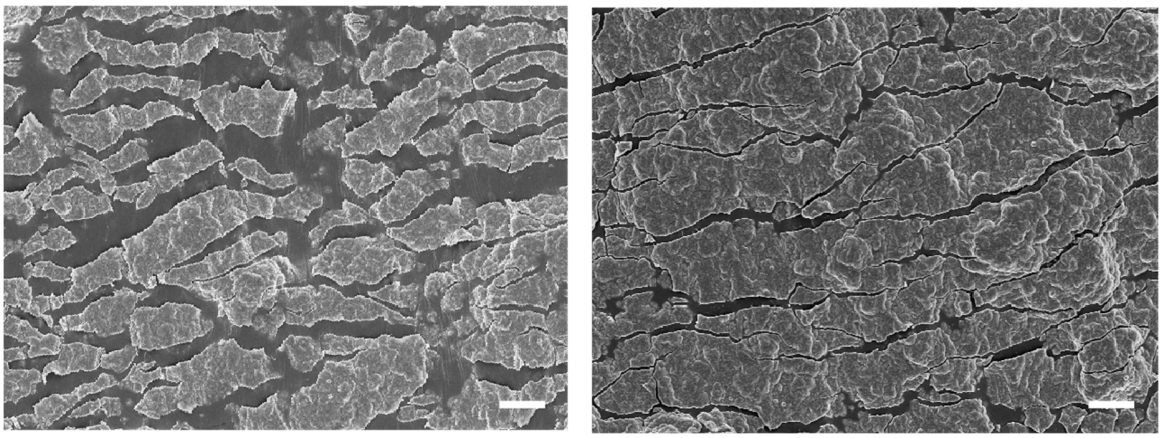

Fig. S12.

Microstructure of microcracked PEDOT: PSS interface layer. SEM images acquired at 150% strain (left) and after full relaxation (right). Scale bars: 10 μm.

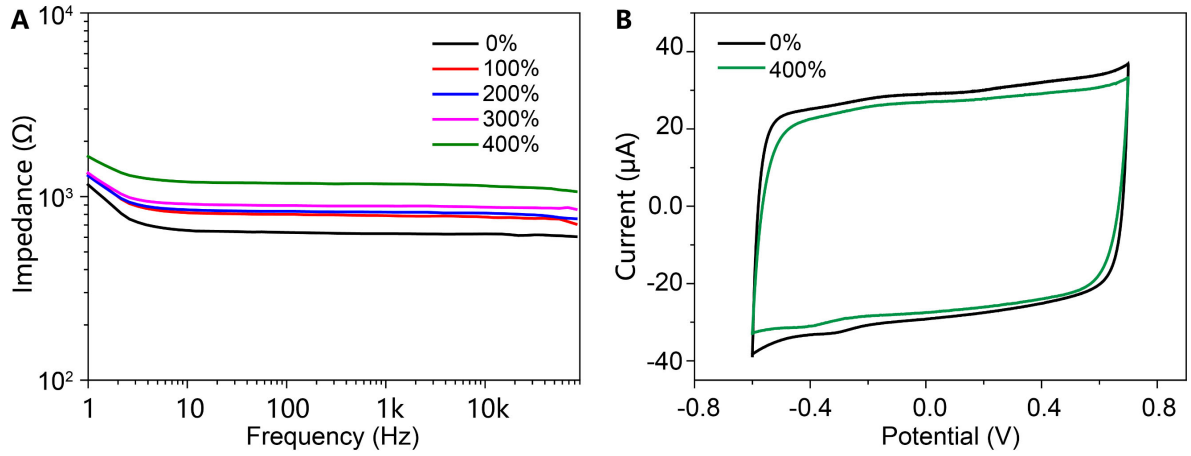

Fig. S13.

Individual sensing channel on the electronic patch under uniaxial tensile deformations. (**A**) Impedance spectra at different tensile strains. (**B**) Cyclic voltammograms at 0 % and the 400 % tensile strains.

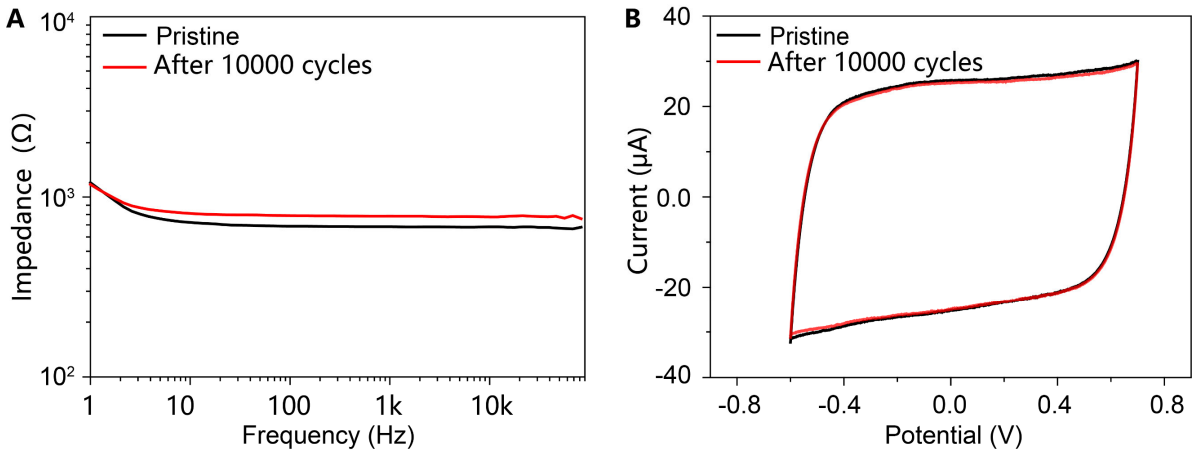

Fig. S14.

Individual sensing channel on the electronic patch in response to tensile fatigue tests. (**A**) Impedance spectra at the pristine state and after 10000 stretch-relaxation cycles (100% strain). (**B**) Cyclic voltammograms at the pristine state and after 10000 stretch-relaxation cycles.

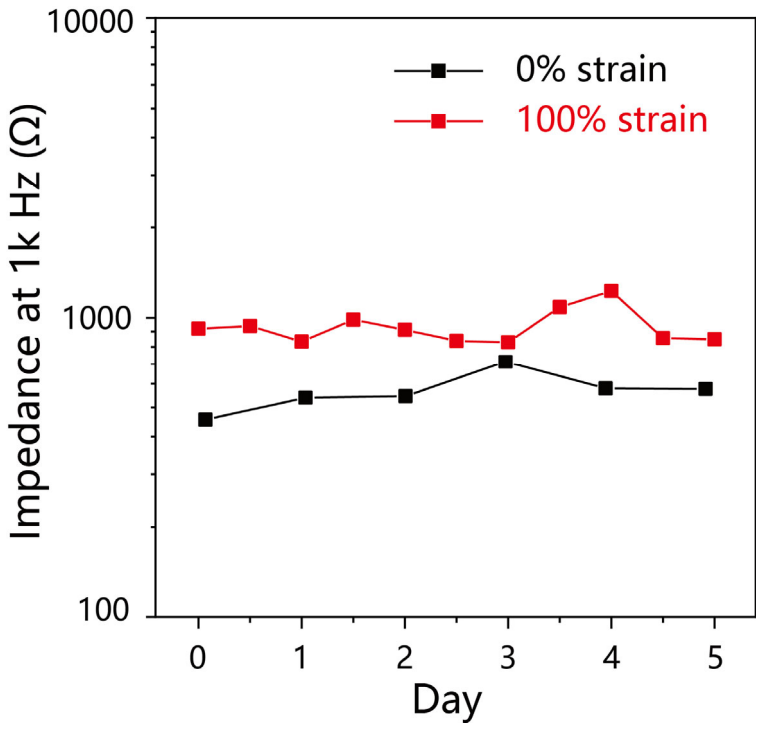

Fig. S15.

Long-term stability of the stretchable electronic patch in PBS solution. Impedance (at 1 kHz) of individual channel on relaxed (0% strain) and stretched (100% strain) patches as a function of storage time.

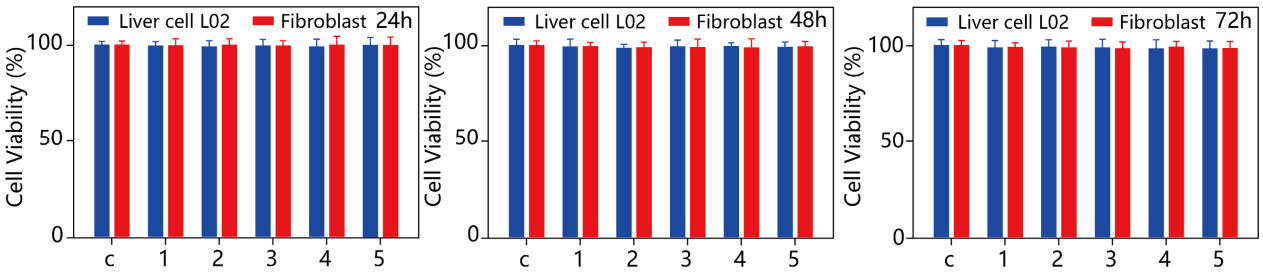

Fig. S16.

***In vitro* biocompatible tests.** Cell viability of L02 and Fibroblast cells after 24 h (left), 48 h (middle), and 72 h (right) incubation with different samples, including normal medium (c), hydrogel adhesive (1), MWCNT nanocomposite (2), PEDOT: PSS (3), SEBS elastomer (4), and as-prepared electronic patch (5). All evaluated materials are potentially in contact with biological tissues during implantable applications. The liquid metal features are well encapsulated and thereby excluded in the assessment. The cell viability analysis on the integrated electronic patch further ensures the lack of toxic leachates during long-term culture.

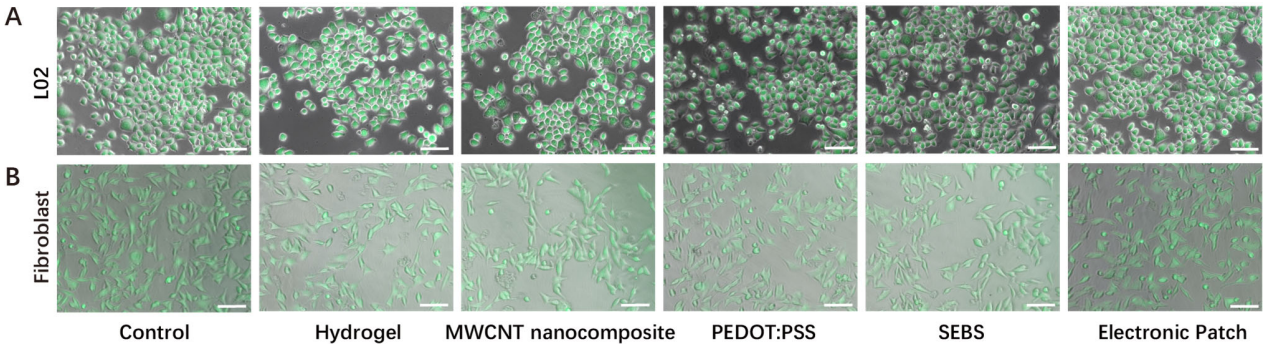

Fig. S17.

Fluorescent microscopy images for cell viability analyses. The L02 and Fibroblast cells have been cultured in growth medium for 72 h together with hydrogel adhesive, MWCNT nanocomposite, PEDOT: PSS, SEBS, and as-prepared electronic patch. The control groups indicate cells in normal growth medium. All cells have been stained with Calcein AM dye for live/dead discrimination. Scale bar: 50 μm.

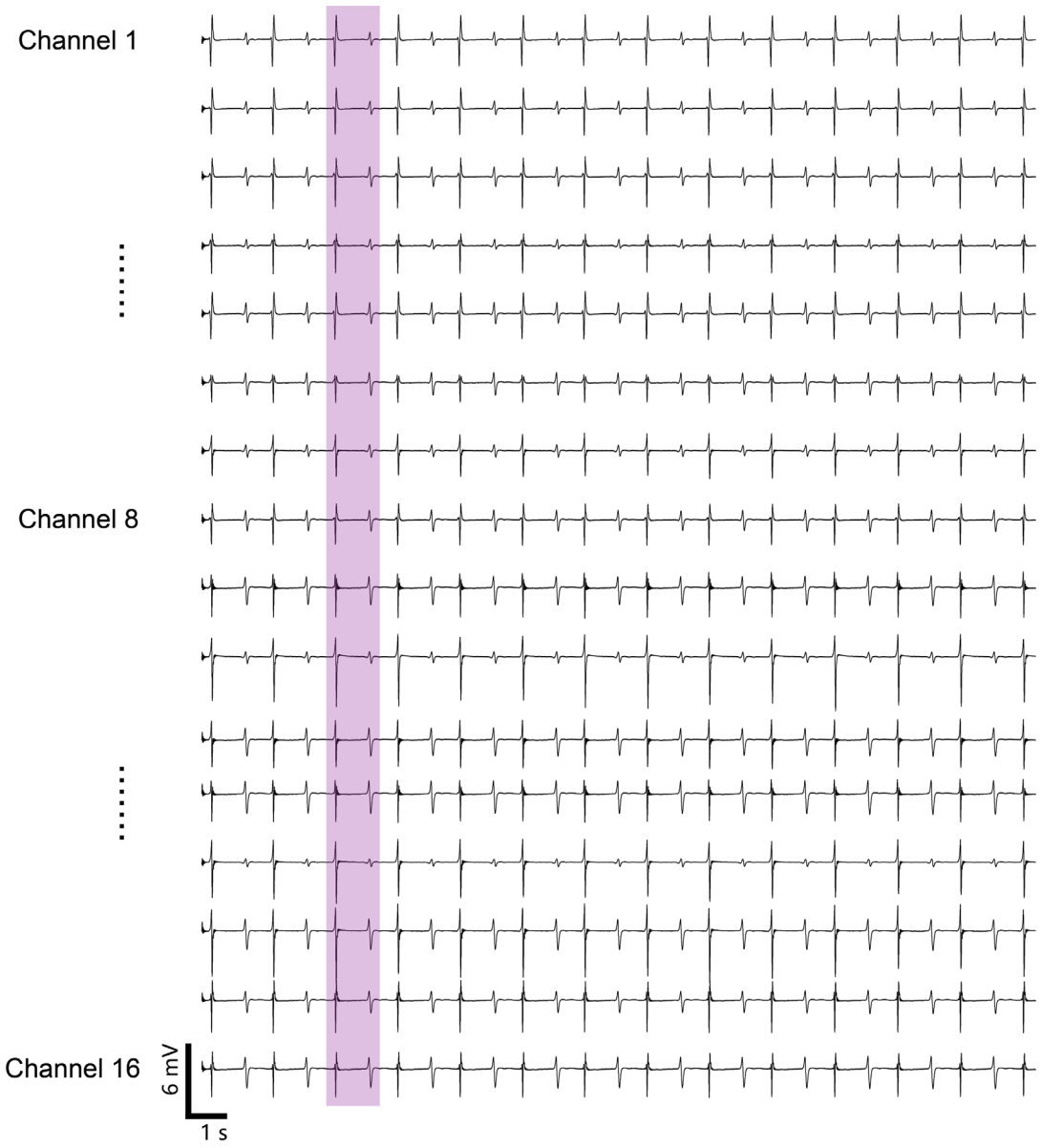

Fig. S18.

16-channel epicardial electrograms acquire from a stretchable electronic patch directly attached to a bullfrog heart. The different waveforms (highlighted by the purple area) reveal the temporally varying potential distribution on the epicardium.

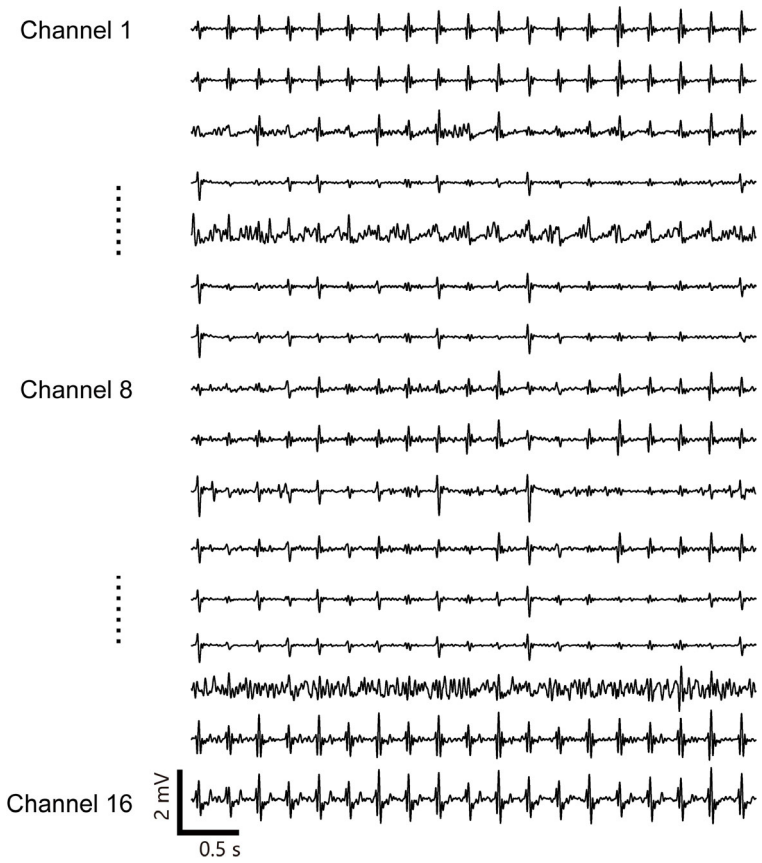

Fig. S19.

16-channel epicardial electrograms acquired from an electronic patch directly attached to a rabbit heart. In Channel 14, the signal is fully covered up by the high noise level and likely associated with the poor contact with the epicardium.

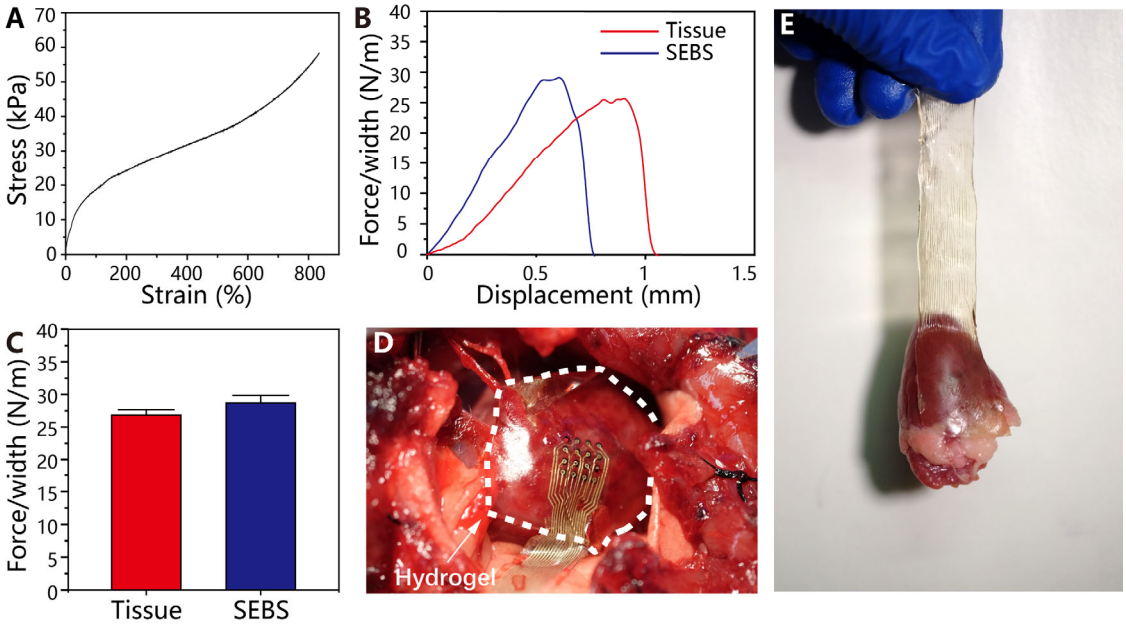

Fig. S20.

Physical properties of polydopamine–polyacrylamide hydrogel adhesive. (**A**) Optical image a chicken heart lifted up by the hydrogel to reveal the strong tissue adhesion. (**B**) As-prepared electronic patch conformally attached to the right ventricle of a rabbit heart by using an additional hydrogel adhesive. The hydrogel is marked by the white dotted line. (**C**) Stress-strain curve of the hydrogel adhesive under uniaxial tensile stretching. (**D**) Force-displacement curves of the hydrogel adhesive on porcine heart tissue and SEBS elastomer under 90 degree peel configuration. (**E**) Corresponding adhesive forces.

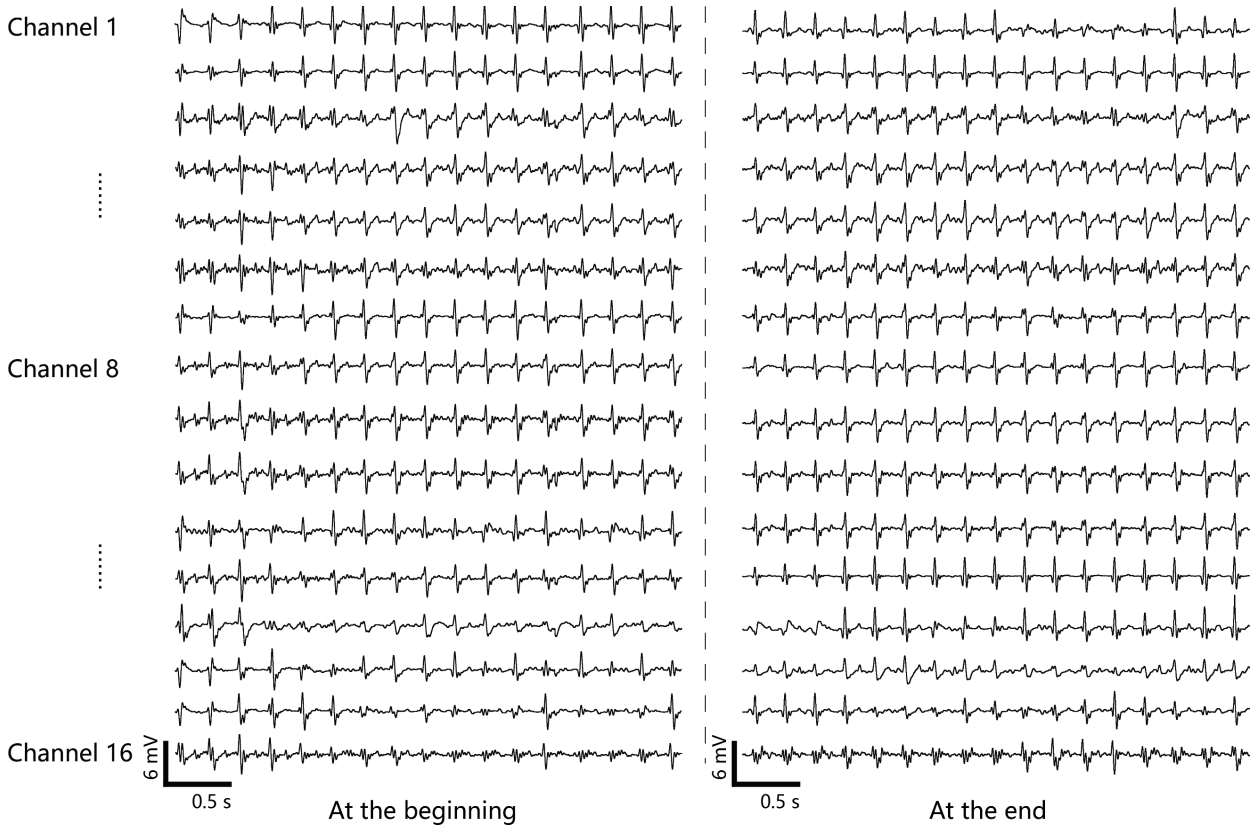

Fig. S21.

16-channel epicardial electrograms acquired from a stretchable electronic patch with conformal and stable attachment to a rabbit heart. An additional hydrogel adhesive has been employed to ensure strong electromechanical coupling. The epicardial electrograms are acquired at the beginning and at the end of a 20 min recording.

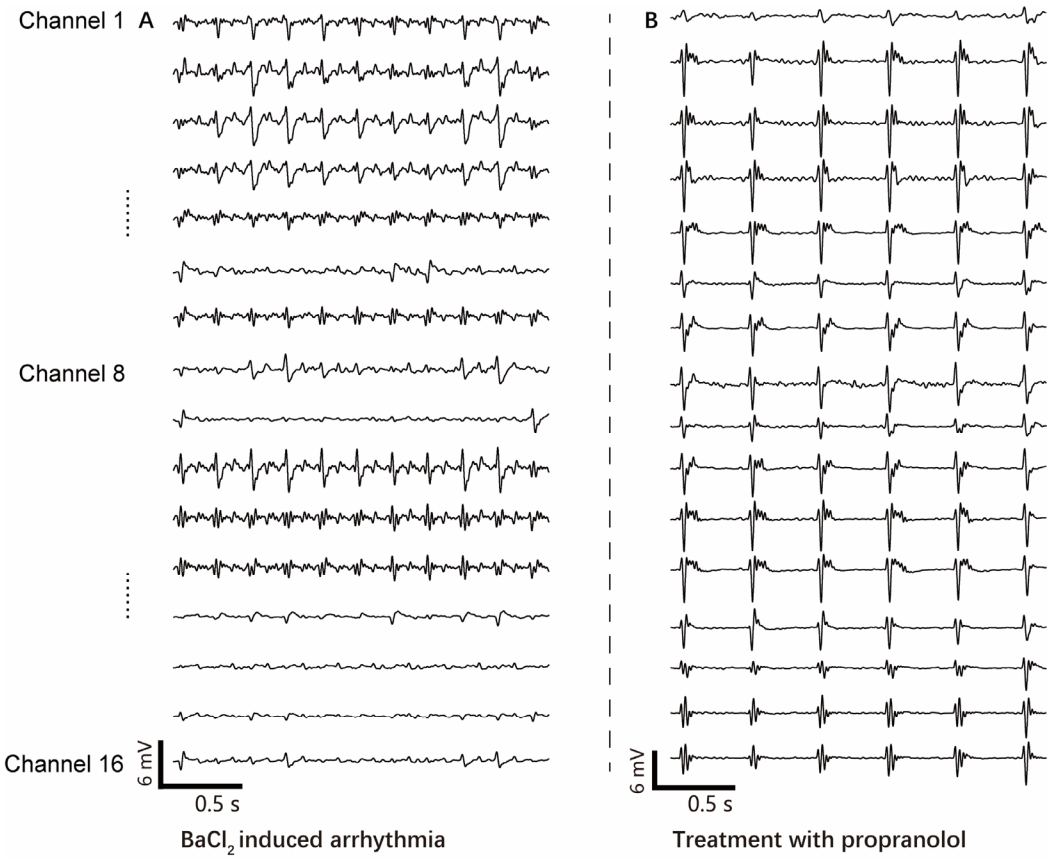

Fig. S22.

16-channel epicardial electrograms of a rabbit under drug-induced arrhythmia and propranolol therapy. (**A**) Epicardial electrograms for cardiac arrhythmia established by intravenous administration of a $BaCl_2$ solution. (**B**) Epicardial electrograms for partially recovered condition after intravenous administration of a propranolol solution. A significant bradycardia is observed as a side effect of the treatment. Notice that an additional hydrogel adhesive has been employed to secure the stretchable electronic patch on the rapidly beating heart.

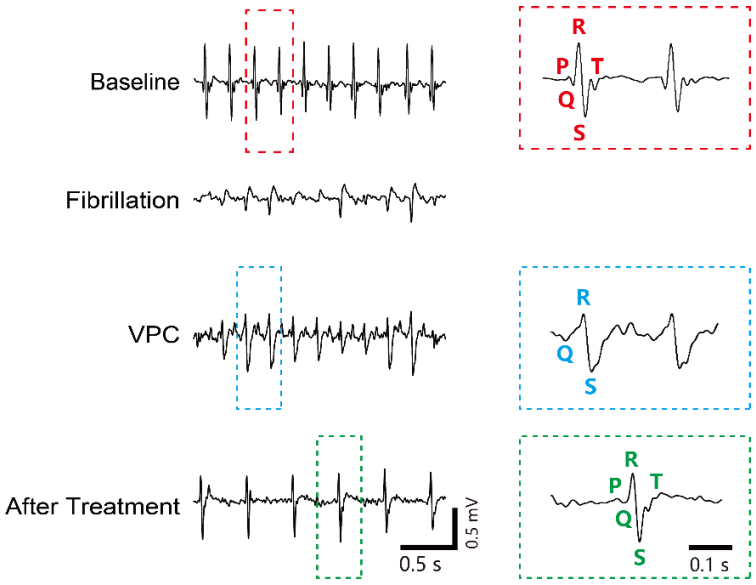

Fig. S23.

Epicardial electrograms for different heart conditions. Characteristic electrograms are shown for normal sinus rhythm, drug-induced cardiac fibrillation, drug-induced ventricular premature contraction (VPC), and propranolol therapy.

Table S1.
A summary of stretchable electronic devices for cardiac applications.

	Maximum strain	Mechanical durability	SNR	Animal	Disease model	Conductor	Design	Reference
Nancomposite cadiac mesh	100%	3000 cycles (30% strain)	NA	Porcine	Acute ischaemia	Ag–AuNW	Stretchable materials	Ref 30
Elastic electrode array	20%	10000 cycles (20% strain)	NA	Pocine	Atrial fibrillation	Au/PEDOT: PSS	Stretchable materials	Ref 17
Rubbery patch	30%	NA	NA	Porcine	NA	AgNW/PDMS	Stretchable materials	Ref 25
Stretchable electronic patch	400%	10000 cycles (100% strain)	48.4 dB	Bullfrog	NA	EGaIn	Stretchable materials	This work
3D integumentary membrane	10%	NA	45 dB	Rabbit (perfusion)	Arrested heart	Cr/Au	Stretchable structures	Ref 11
Nancomposite cadiac mesh	NA	NA	20.1 dB	Rat	Fibrillation/ Myocardial infarction	Ag–AuNW	Stretchable materials	Ref 27
Elastic electrode array	20%	10000 cycles (20% strain)	40.2 dB	Rabbit	NA	Au/PEDOT: PSS	Stretchable materials	Ref 17
Ultraflexible multielectrode arrays	15%	NA	52 dB	Rat	NA	Au	Stretchable structures	Ref 19
Stretchable electronic patch	400%	10000 cycles (100% strain)	42.7 dB	Rabbit	Arrhythmia	EGaIn	Stretchable materials	This work

*The blue color denotes low heart rate models (<100 bpm). The red color represents high heart rate models (>120 bpm).

Movie S1.

A representative stretchable electronic patch with conformal attachment to a beating bullfrog heart for biopotential recording/mapping.

Movie S2.

A representative stretchable electronic patch with stable coupling to a beating rabbit heart by using an additional hydrogel adhesive.